Supporting Information

Precise Graphitic Nitrogen-Incorporation by Electrochemical Oxidation

Leilei Xu [a], Zhibo Zhang [a], Hong Zhou [b], Ziqi Wen [c], Yuxuan Liu [a], Heng Dong [a] *, Wei Xie [b] *

[a] MOE Key Laboratory of Pollution Processes and Environmental Criteria, College of Environmental Science and Engineering, Nankai University, Tianjin 300350, China.

[b] State Key Laboratory of Advanced Chemical Power Sources, Key Laboratory of Advanced Energy Materials Chemistry (Ministry of Education), Tianjin Key Lab of Biosensing & Molecular Recognition, Haihe Laboratory of Sustainable Chemical Transformations, Renewable Energy Conversion and Storage Center, College of Chemistry, Nankai University, Tianjin 300071, China.

[c] College of Materials Science and Engineering, Nankai University, Tianjin 300350, China.

Table of content

Materials and Methods

Materials

Graphite paper and graphene oxide quantum dots were sourced from Jiangsu Xianfeng Nano. Sodium nitrate ($NaNO_3$, 98%), ammonium sulfate ($(NH_4)_2SO_4$, AR), sodium sulfate (Na_2SO_4, 99%), zinc chloride ($ZnCl_2$, AR), iron chloride ($FeCl_3$, 99%), and methanol (MeOH, AR) were from Aladdin Chemical (Shanghai, China). Sulfuric acid (H_2SO_4, 99%) and hydrochloric acid (HCl, 99%) were from Bohua Reagent (Tianjin, China). PDS (99%) was purchased from J&K Scientific.

Apparatus and measurements

Aberration Corrected Transmission Electron Microscope was employed on a JEM-ARM200F. Transmission electron microscope (TEM) images and elemental analysis of the nanostructures were carried out on a high-resolution transmission electron microscope FEI Talos F200X G2, operating at a voltage of 200 kV. The XRD data were collected using a Rigaku SmartLab 9KW θ/θ diffractometer with a Cu Kα source. The wide angle XRD scans from 5° to 80° with the step size of 0.020° and scan rate of 0.125°/s. Elemental composition and chemical structure of g-ENGO were detected by X-ray photoelectron spectroscopy (XPS, Thermo ESCALAB250XI) with an Al Kα X-ray source and an elemental analyzer (LEEMANEA3000). Defect level in the material was evaluated by Raman spectroscope (Renishaw 1000NR) with excitation of 532 nm laser light. The carbon vacancy content in EGO and nitrogen radicals in the system were measured using an electron paramagnetic resonance spectrometer (EPR, Bruker EMX Xplus-10/12, microwave frequency = 9.853 GHz, microwave power = 20 mW, modulation amplitude = 1 G, modulation frequency = 100 kHz). Electrochemical tests were performed on an electrochemical workstation (Chenhua CHI660D) with a three-electrode system. The gas generated by carbon vacancy escape was detected using in situ differential electrochemical mass spectrometry (DEMS, LingLu QAS100), which was equipped with an electrochemical workstation (Chenhua CHI660D) and a peristaltic pump (flow rate 3 mL/min). In surface-enhanced Raman scattering (SERS) testing, Raman spectra were collected using a confocal Raman microscope (Horiba LabRAM HR Evolution) with a water immersion Olympus objective (40×, WD = 3.3 mm). The in-situ Raman cell was purchased from BEIJING SCISTAR TECHNOLOGY CO. LTD.

Synthetic methods

The Synthesis of the EGO

In a three-electrode electrochemical system, Pt is used as the counter electrode, Ag/AgCl as the reference electrode, graphite paper (1.5 cm × 0.8 cm× 0.02 mm) as the working electrode, and sulfuric acid (H_2SO_4, 50 wt.%) as the electrolyte. At a constant potential of 1.8 V, the electrochemical oxidation of graphene can be completed within 30 min, and the resulting product is denoted as EGO.

The Synthesis of the g-ENGO

In a three-electrode electrochemical system, Pt is used as the counter electrode, and Ag/AgCl is used as the reference electrode. EGO obtained by oxidation is used as the working electrode, and 1.25 M $(NH_4)_2SO_4$ is used as the electrolyte. After oxidation for 30 min at a constant potential of less than 1.8 V, graphite nitrogen-doped graphene oxide is obtained, denoted as g-ENGO.

The Synthesis of the g-ERNGO

In a three-electrode electrochemical system, Pt is used as the counter electrode, Ag/AgCl as the reference electrode, g-ENGO as the working electrode, and 0.5 M Na_2SO_4 as the electrolyte. After reduction for 30 min at a constant potential of -1.2 V, graphite nitrogen-doped reduced graphene oxide (g-ERNGO) is obtained.

Operando electrochemical characterization

Operando EPR measurement of free radicals

To investigate the generation of nitrogen, hydroxyl, and sulfate radicals at the electrochemically oxidized anode, linear sweep voltammetry (LSV) was coupled with in situ electron paramagnetic resonance (EPR) spectroscopy. The spin-trapping agent 5,5-dimethyl-1-pyrroline-N-oxide (DMPO) was employed to enhance signal intensity and facilitate radical identification. Experiments were carried out in a combined electrochemical–EPR cell that enabled simultaneous electrochemical reaction and EPR signal acquisition. Graphite paper, a platinum wire, and a saturated Ag/AgCl (3.0 M KCl) electrode were used as the working, counter, and reference electrodes, respectively. The electrolyte was a 1.25 M aqueous solution of $(NH_4)_2SO_4$. Before measurements, all solutions were purged with high-purity N_2 for 30 min to remove dissolved O_2. Electrochemical experiments were performed using a CHI660D electrochemical workstation over a potential range of 0–1.8 V (vs Ag/AgCl) at a scan rate of 1 $mV \cdot s^{-1}$. EPR spectra were acquired synchronously during the LSV scan under the following conditions: microwave frequency = 9.853 GHz, microwave power = 20 mW, modulation amplitude = 1 G, modulation frequency = 100 kHz, time constant = 0.1 s, and acquisition time = 60 s per spectrum.

Operando DEMS testing

Electrochemical oxidation of graphite in sulfuric acid was investigated using linear sweep voltammetry (LSV) coupled with differential electrochemical mass spectrometry (DEMS). The DEMS flow cell equipped with a gas-permeable polytetrafluoroethylene (PTFE) membrane enabled direct transfer of gaseous products from the electrode surface to the mass spectrometer. Graphite paper, a platinum wire, and a saturated Ag/AgCl (3.0 M KCl) electrode were used as the working, counter, and reference electrodes, respectively. The electrolyte consisted of 50 wt.% H_2SO_4. All solutions were purged with high-purity argon for at least 30 min prior to testing to eliminate dissolved oxygen. LSV scans were performed using a CHI660D electrochemical workstation over a potential range of 0–1.8 V (vs Ag/AgCl) at a scan rate of 10 $mV \cdot s^{-1}$ and repeated 10 times. CO and CO_2 generated during anodic polarization were detected in real time by monitoring the m/z = 28 and m/z = 44 signals, respectively.

Operando SERS testing

Synthesis of Au nanoparticles (~80 nm)

Au NPs were synthesized following a reported protocol[1, 2]. Initially, 0.15 L of 2.2 mM sodium citrate (SC) solution was heated to boiling in a 0.25 L flask under continuous stirring. After a short reflux period, 850 μL of 1% $HAuCl_4$ solution was rapidly injected to form ~10 nm gold seeds. Once the solution color changed from colorless to pink, it was cooled to 90°C, followed by the rapid addition of another 850 μL of 1% $HAuCl_4$. After 30 min, a third aliquot of 850 μL of 1% $HAuCl_4$ was added, and the reaction was maintained for an additional 30 min. Subsequently, 55 mL of the solution was removed, and 2 mL of 60 mM SC solution along with 53 mL of deionized water was added to restore the total volume. This diluted mixture was used as the seed solution, and the particle growth cycle was repeated until AuNPs with a diameter of ~80 nm were obtained.

Synthesis of Au@SiO2 shell-core structures

To the centrifuged Au NP suspension, sequentially add 10 μL of 1% SC solution and 10 μL of 10% MPTMS ethanol solution. Stir the mixture at 50°C and 53 rcf for 1 hour using a mixing instrument, then wash twice with water via centrifugation–redispersion cycles. Subsequently, add 15 μL of 0.054% sodium silicate solution to 985 μL of the suspension, dilute the mixture at a 1:10 ratio, and centrifuge at 90°C and 53 rcf for 1 h. After removing the supernatant, the $Au@SiO_2$ composite particles are obtained and ready for use.

SERS structure assembly

The synthesized $Au@SiO_2$ composite particles were dispersed in deionized water, while graphene oxide quantum dots (GOQDs), containing carbon vacancies as confirmed by electron paramagnetic resonance (EPR), were dispersed in ethanol. Under ultrasonic agitation, the ethanol dispersion of GOQDs was slowly injected into the aqueous dispersion of $Au@SiO_2$ at a volume ratio of 1:1 to achieve heterostructure assembly. The assembled product was collected by centrifugation (114 rcf, 10 min), washed, and re-dispersed in ethanol for subsequent use.

Electrode preparation

A small aliquot of the ultrasonically mixed SERS heterostructure was drop-cast onto the surface of a glassy carbon electrode (GCE). The electrode was then irradiated with infrared light to form a uniform coating film and dried under ambient conditions prior to electrochemical measurements.

In-situ surface-enhanced Raman spectroscopy (SERS) measurements

Raman spectroscopy was conducted using a confocal Raman microscope equipped with a 50× objective lens and an excitation wavelength of 633 nm. The in situ electrochemical Raman cell consisted of a membrane-coated GCE as the working electrode, an Ag/AgCl reference electrode, and a platinum wire counter electrode. Electrochemical oxidation was performed on a workstation in the staircase electrochemical potential (STEP) mode, with the potential increasing from 0.8 to 1.95 V in 0.5 V increments, and an oxidation duration of 120 s at each step. Raman spectra were recorded simultaneously at each potential, and the total experiment time was 1440 s.

Density functional theory calculation method

All density functional theory (DFT) calculations were conducted using Gaussian methods. Geometry optimizations of all molecules were performed with the M06-2X functional[3] and the def2-SVP basis set[4] and single point calculations with the def2-TZVP basis set. The vibrational frequencies of all species were calculated at the same level and it was ensured that there existed one and only one imaginary frequency in the transition state structures.

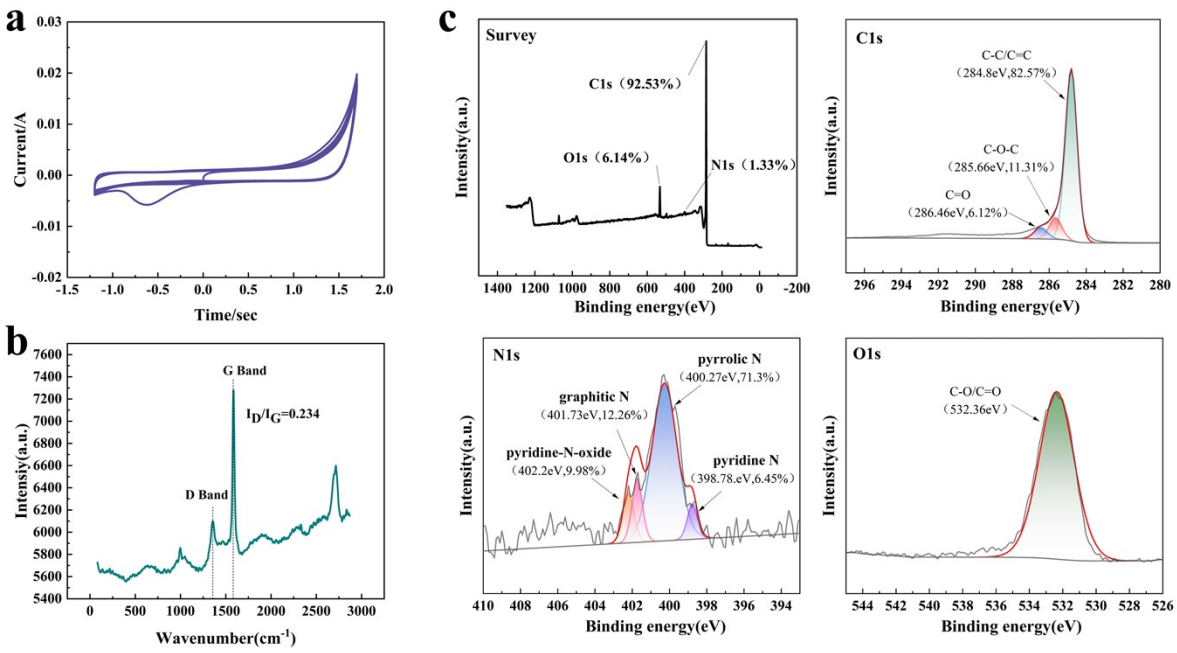

Fig. S1. (a) Cyclic voltammetry. (b) Raman spectra of g-ENGO. (c) XPS spectrum for Survey, C1s, N1s, and O1s of g-ENGO.

Graphite electrodes were subjected to electrochemical treatment in 1.25 M $(NH_4)_2SO_4$ solution, and graphene-enhanced nitrogen-doped graphene (g-ENGO) was prepared via cyclic voltammetry[5, 6] under potential conditions. Under room temperature (25°C) conditions, cyclic testing was conducted at a scan rate of 50 mV/s over a variety of cycles (from 1 to 100), with the test potential range spanning from -1.2 V to +1.7 V relative to Ag/AgCl (dissolved in 3 M potassium chloride). As can be seen from the XPS test results, this method can only produce graphene doped with pyridine nitrogen, pyrrole nitrogen, and graphite nitrogen, and it isn't easy to control the content of a single graphite nitrogen.

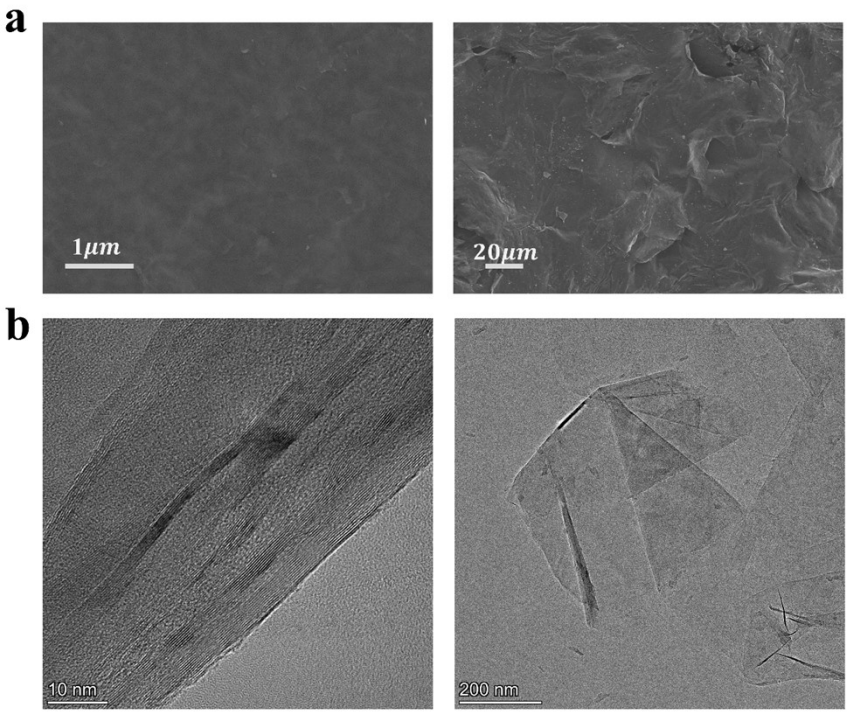

Fig. S2. (a) SEM images, and (b) TEM images of g-ENGO.

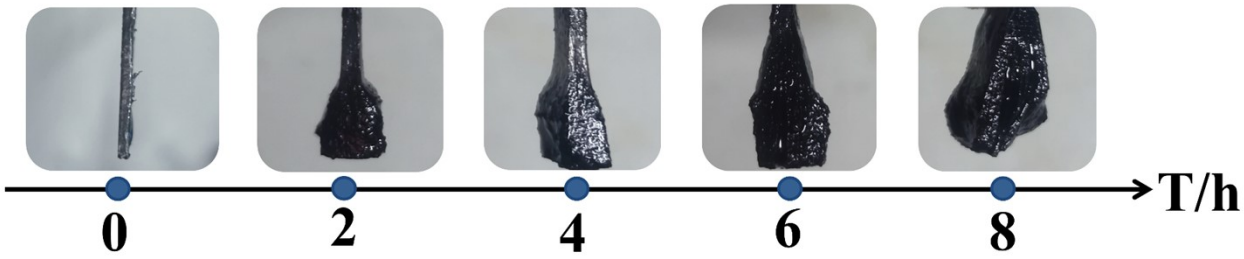

Fig. S3. Optical images of 1 mm thick graphite paper electrochemically oxidized for 2 h, 4 h, 6 h, and 8 h.

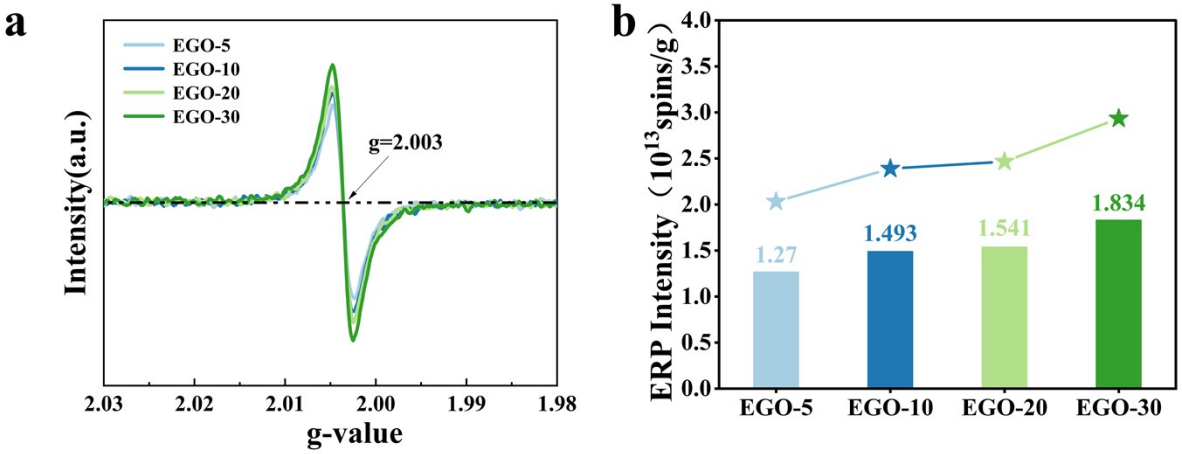

Fig. S4. (a) EPR spectra of EGO. (b) Carbon vacancy intensity.

In a three-electrode electrochemical system, H_2SO_4 (50 wt.%) is used as the electrolyte, platinum wire as the counter electrode, and Ag/AgCl as the reference electrode. Graphite paper with a thickness of 0.02 mm is used as the working electrode. It is oxidized at a voltage of 1.8 V for 5 min, 10 min, 20 min, and 30 min, respectively, denoted as EGO-5, EGO-10, EGO-20, and EGO-30. The carbon vacancy content of EGO is determined using EPR spectroscopy[7].

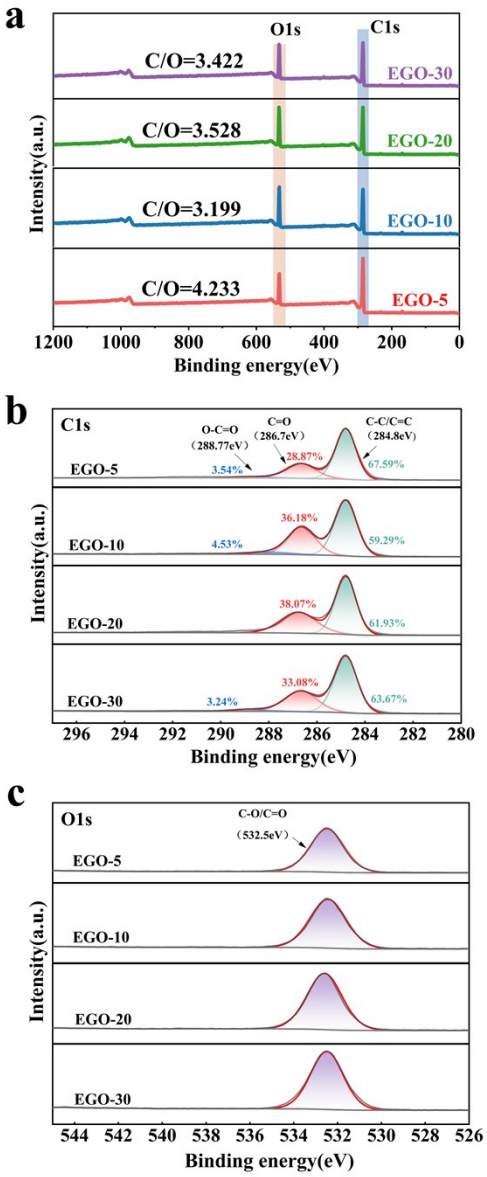

Fig. S5. High-resolution XPS (a) Survey(C/O), (b) C1s, and (c) O1s spectra of EGO.

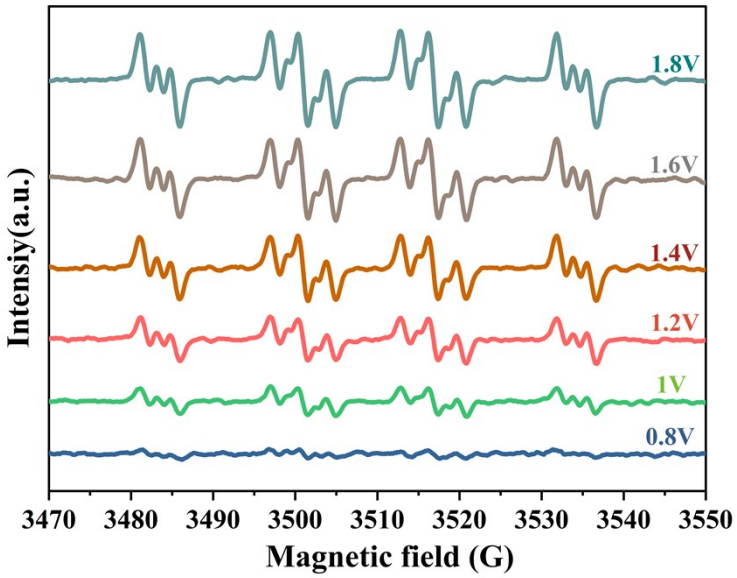

Fig. S6. Operando EPR spectra of DMPO-N during g-ENGO preparation.

In a three-electrode electrochemical system, a platinum wire was employed as the counter electrode, and Ag/AgCl was used as the reference electrode. Graphite paper (0.02 mm thick) was used as the working electrode (free from carbon vacancies), and a 1.25 M $(NH_4)_2SO_4$ solution served as the electrolyte. The system was continuously oxidized for 30 min at various voltages (0.8 V, 1.0 V, 1.2 V, 1.4 V, 1.6 V, 1.8 V). During this process, DMPO was added to capture N radicals in real time. EPR spectra[8] revealed that the number of N radicals generated at the anode increased with the applied potential.

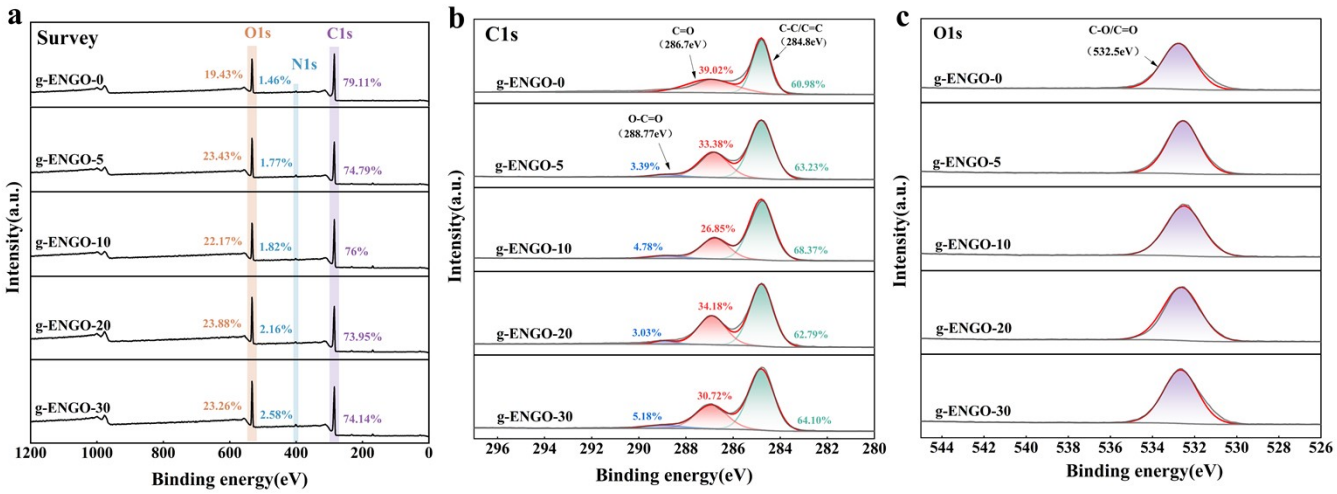

Fig. S7. High-resolution XPS (a) Survey, (b) C1s, and (c) O1s spectra of g-ENGO-x (x represents different oxidation times).

In a three-electrode electrochemical system, a platinum wire served as the counter electrode, and Ag/AgCl was used as the reference electrode. Initially, in a 50 wt.% H_2SO_4 electrolyte, a 0.02 mm thick graphite paper was employed as the working electrode. Oxidation was performed at 1.8 V for various durations (0, 5, 10, 20, and 30 min), yielding the samples denoted as EGO-0, EGO-5, EGO-10, EGO-20, and EGO-30, respectively. Subsequently, these six EGO samples were used as working electrodes, and the system was continuously oxidized in a 1.25 M $(NH_4)_2SO_4$ electrolyte at 1.8 V for 1 h to obtain g-ENGO-x (where x represents the oxidation time). The resulting g-ENGO samples were characterized using X-ray photoelectron spectroscopy (XPS).

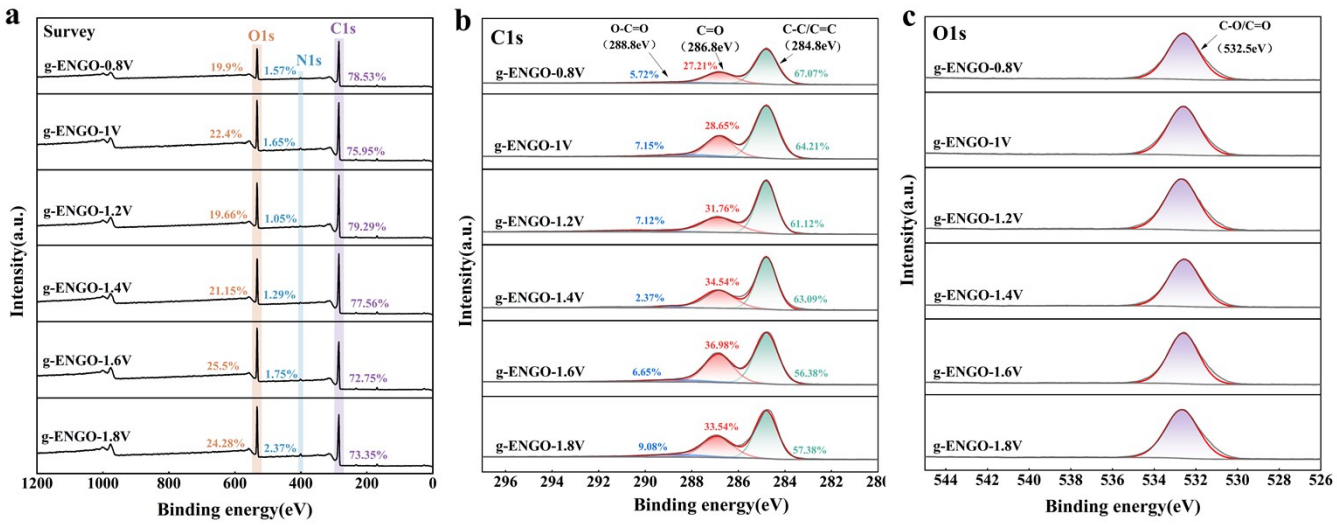

Fig. S8. High-resolution XPS (a) Survey, (b) C1s, and (c) O1s spectra of g-ENGO-x (x represents different doping potentials).

In a three-electrode electrochemical system, a platinum wire served as the counter electrode, and Ag/AgCl was used as the reference electrode. Initially, in a 50 wt.% H_2SO_4 electrolyte, a 0.02 mm thick graphite paper was employed as the working electrode. Oxidation was carried out at 1.8 V for 30 min to obtain EGO-30. Subsequently, EGO-30 was used as the working electrode in a 1.25 M $(NH_4)_2SO_4$ electrolyte, and continuous oxidation was performed at various voltages (0.8 V, 1.0 V, 1.2 V, 1.4 V, 1.6 V, 1.8 V) for 30 min, yielding g-ENGO-x (where x represents the different doping potentials). The resulting g-ENGO samples were characterized by X-ray photoelectron spectroscopy (XPS).

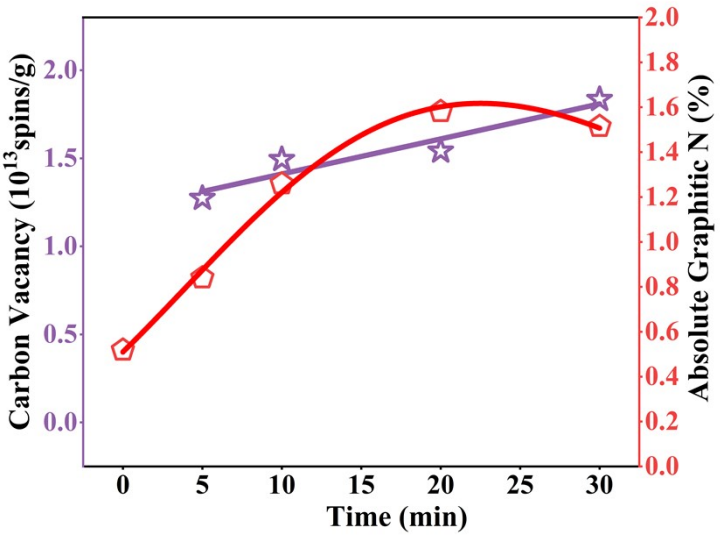

Fig. S9. The relationship between carbon vacancies and absolute graphitic N content as a function of oxidation time.

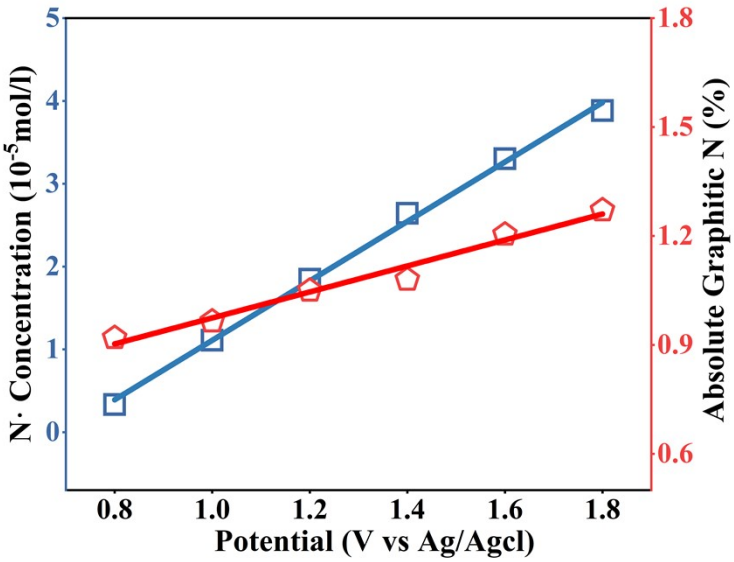

Fig. S10. The relationship between N radicals and absolute graphitic N content as a function of voltage.

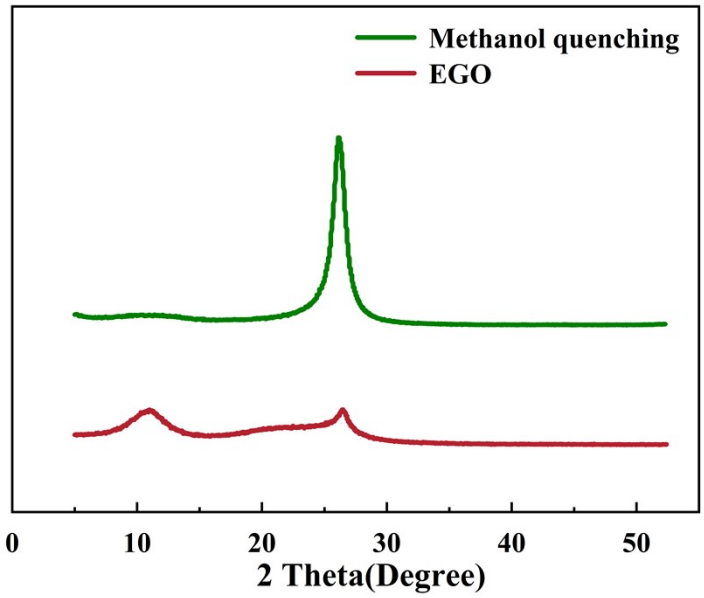

Fig. S11. XRD of EGO and EGO after methanol quenching.

In a three-electrode system, a 1.25 M $(NH_4)_2SO_4$ electrolyte was used. One group was oxidized at 1.6 V for 10 min to obtain EGO, while another group received the addition of 50 mM methanol to the electrolyte to quench hydroxyl radicals. This second group was then similarly oxidized at 1.6 V for 10 min to obtain EGO after methanol quenching. Both sets of samples were characterized by X-ray diffraction (XRD)[9]. EGO exhibited a characteristic diffraction peak corresponding to the (100) crystal plane of oxidized graphene at approximately 10° (2θ), whereas the EGO sample from the quenched system showed a strong peak at around 26.8° (2θ), corresponding to the (002) crystal plane of graphite. Moreover, organic elemental analysis (Table S3) of the EGO from the methanol-quenching system revealed that the nitrogen and oxygen contents were nearly zero, providing clear evidence of the essential role of water decomposition in the formation of oxidized and nitrogen-doped materials.

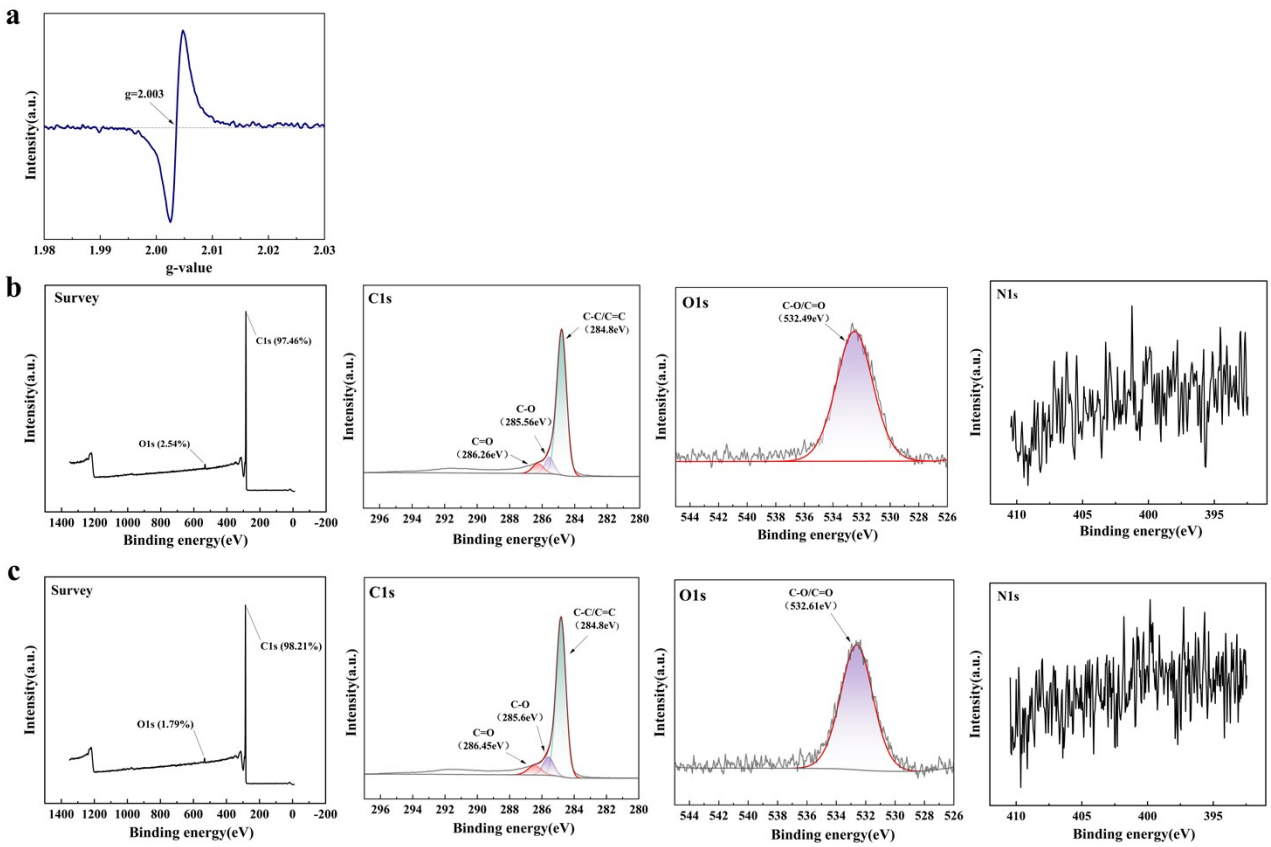

Fig. S12. (a) EPR of GNCV. High-resolution XPS of (b) GPCV, (c) GNPCV.

By introducing an appropriate nitrogen source and subjecting the carbon material to high-temperature pyrolysis, materials containing graphitic nitrogen can be synthesized. This approach has been extensively reported[10, 11]. To investigate this, we designed a comparative experiment. First, graphite powder was washed with deionized water to remove impurities and then dried at 105°C to obtain clean graphite powder. 9 g of the dried sample were sieved through a 60-mesh screen, mixed with 27 g of $ZnCl_2$ and 150 mL of 3 M $FeCl_3$ solution, stirred in a water bath at 80°C for 48 h, and subsequently dried in a forced-air oven at 100°C for 5 days to yield a solid precursor. The precursor was pyrolyzed in an argon atmosphere tube furnace at a heating rate of 5°C min^{-1}, reaching 900°C and maintained for 2 h. The resulting powder was acid-washed with 2 M HCl to remove residual Fe^{3+} and Zn^{2+} ions and then freeze-dried to obtain graphite powder containing carbon vacancies, designated as GPCV. Electron paramagnetic resonance (EPR) characterization of GPCV revealed a high concentration of carbon vacancies. Subsequently, 4.5 g of GPCV underwent the same procedure, with the addition of 9 g of melamine prior to the water bath step, producing a sample labeled GNPCV. X-ray photoelectron spectroscopy (XPS) results before and after pyrolysis indicated that oxygen-containing functional groups are unlikely to form in a high-temperature reducing atmosphere. Moreover, neither the pre- nor post-pyrolysis material contained nitrogen, suggesting that even with abundant carbon vacancies and sufficient nitrogen sources, nitrogen atoms do not readily incorporate into carbon vacancies to form graphitic nitrogen without the presence of oxygen-containing functional groups.

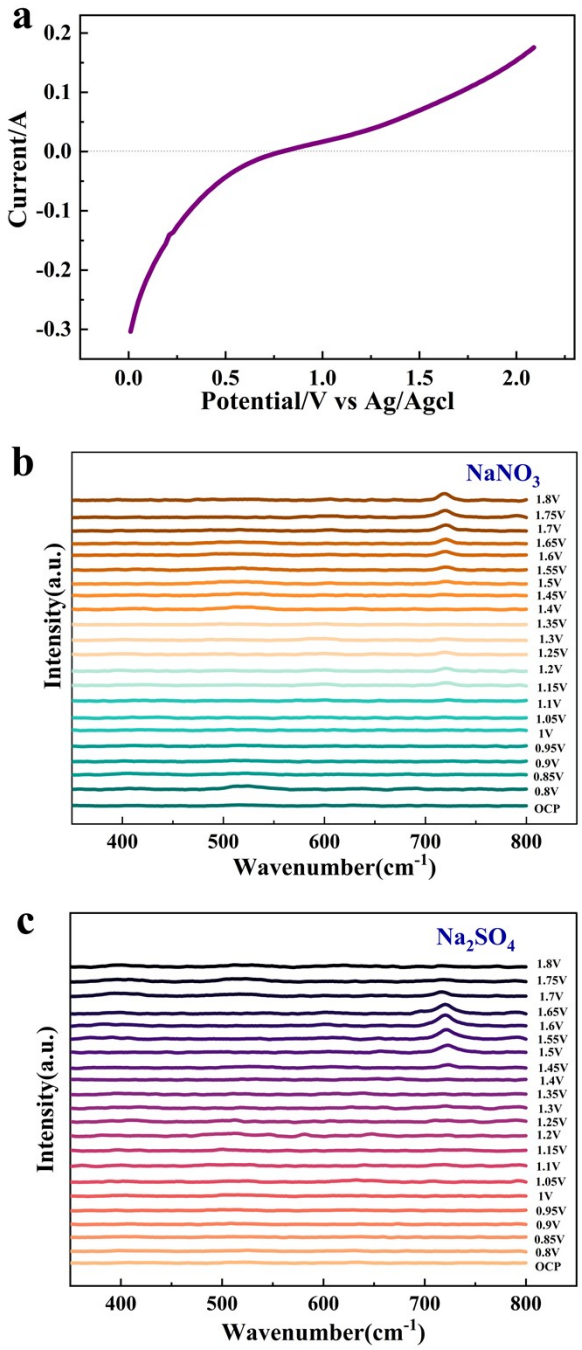

Fig. S13. (a) LSV. (b) SERS spectrum of the anode surface in a 2.5 M $NaNO_3$ aqueous solution. (c) SERS spectrum of the anode surface in a 2.5 M Na_2SO_4 aqueous solution.

SERS spectroscopy showed that no characteristic peaks of N species (410 cm^{-1}, 585 cm^{-1}, 662 cm^{-1}) were observed in sodium sulfate and sodium nitrate solutions.

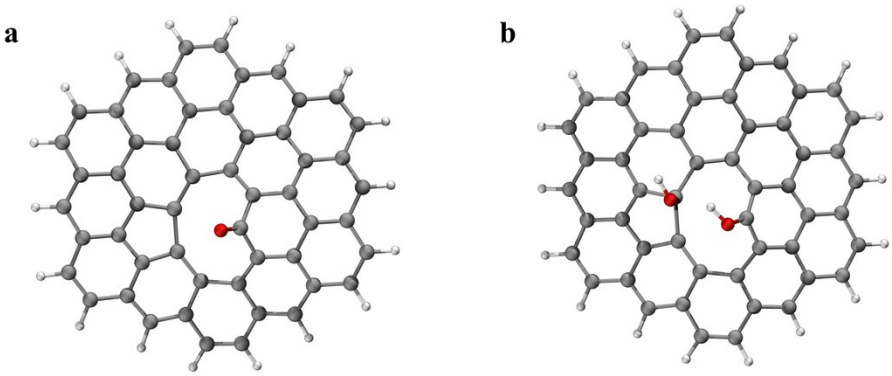

Fig. S14. (a) EG0-1. (b) EGO-2.

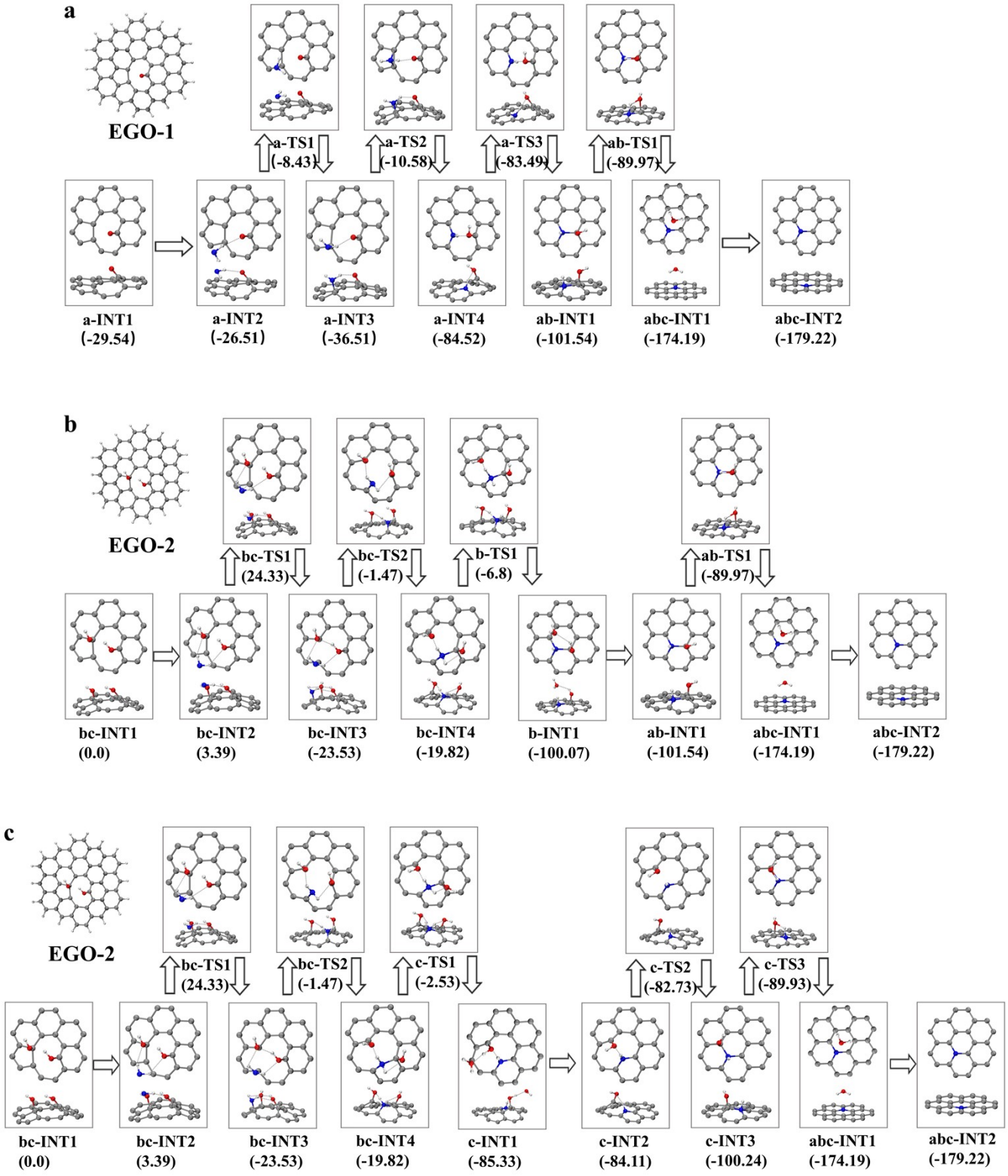

Fig. S15. Fragmental structures for the stationary points involved in (a) route-a, (b) route-b, and (c) route-c. Atom representations are O (red), N (blue), C (gray), and H(white). Other carbon atoms are omitted for clarity.

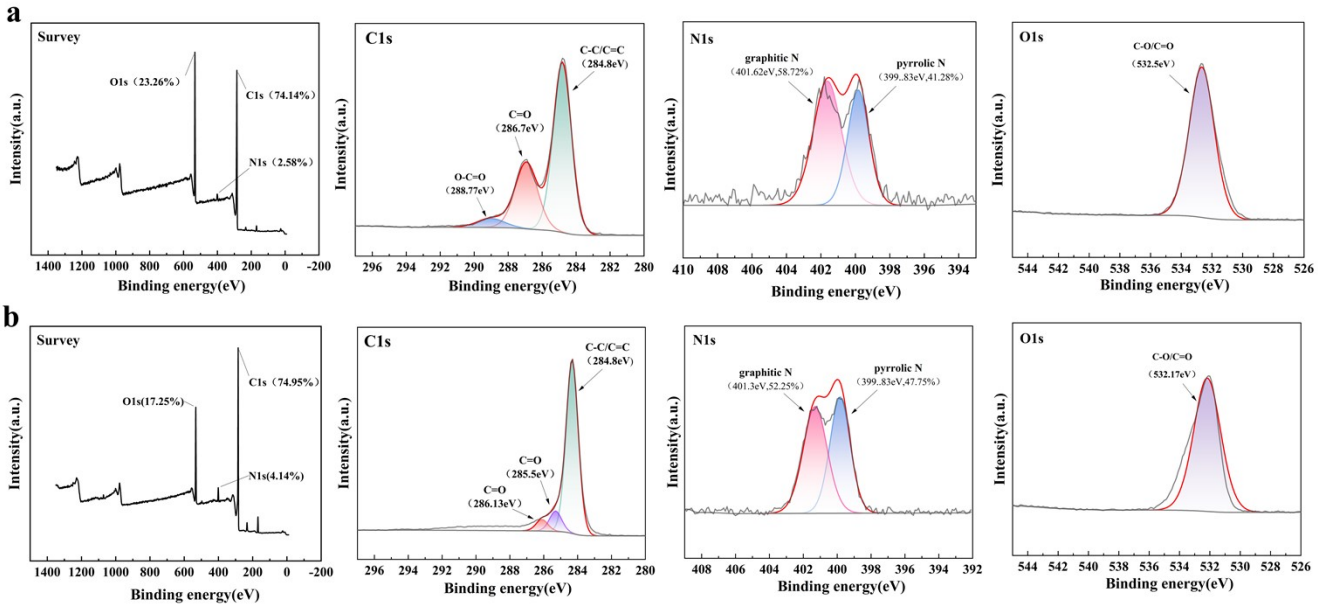

Fig. S16. High-resolution XPS of (a) g-ENGO-30. (b) g-ERNGO.

In a three-electrode electrochemical system, graphite paper with a thickness of 0.02 mm was employed as the working electrode. Initially, the graphite paper was oxidized in a 50 wt.% H_2SO_4 electrolyte at 1.8 V for 30 min to produce EGO-30. Subsequently, EGO-30 was used as the working electrode in a 1.25 M $(NH_4)_2SO_4$ electrolyte and subjected to further oxidation at 1.6 V for 1 h, yielding g-ENGO-30. Finally, g-ENGO-30 underwent electrochemical reduction in a 0.5 M Na_2SO_4 electrolyte at –1.2 V for 30 min to obtain g-ERNGO. X-ray photoelectron spectroscopy (XPS) analysis of g-ENGO-30 and g-ERNGO indicated that the relative content of graphitic nitrogen remained nearly unchanged following the reduction process, whereas the total nitrogen content increased.

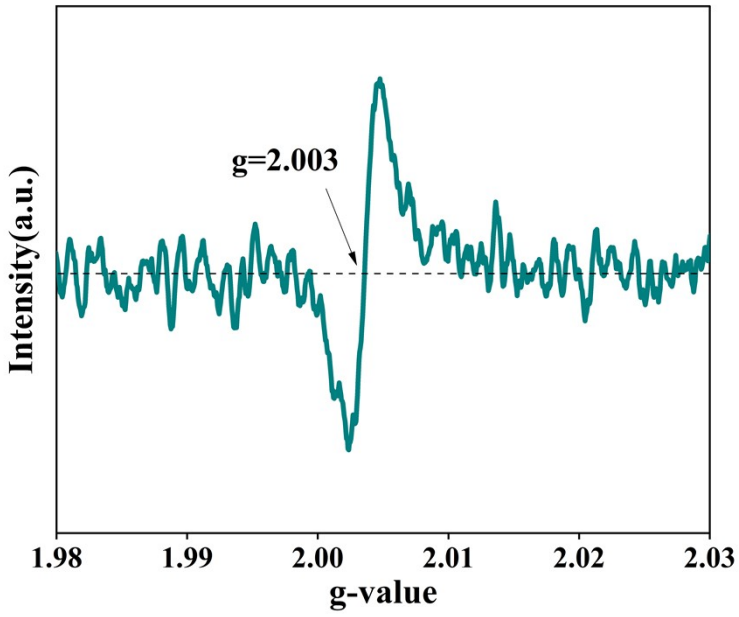

Fig. S17. EPR of graphene oxide quantum dots (GOQD).

.

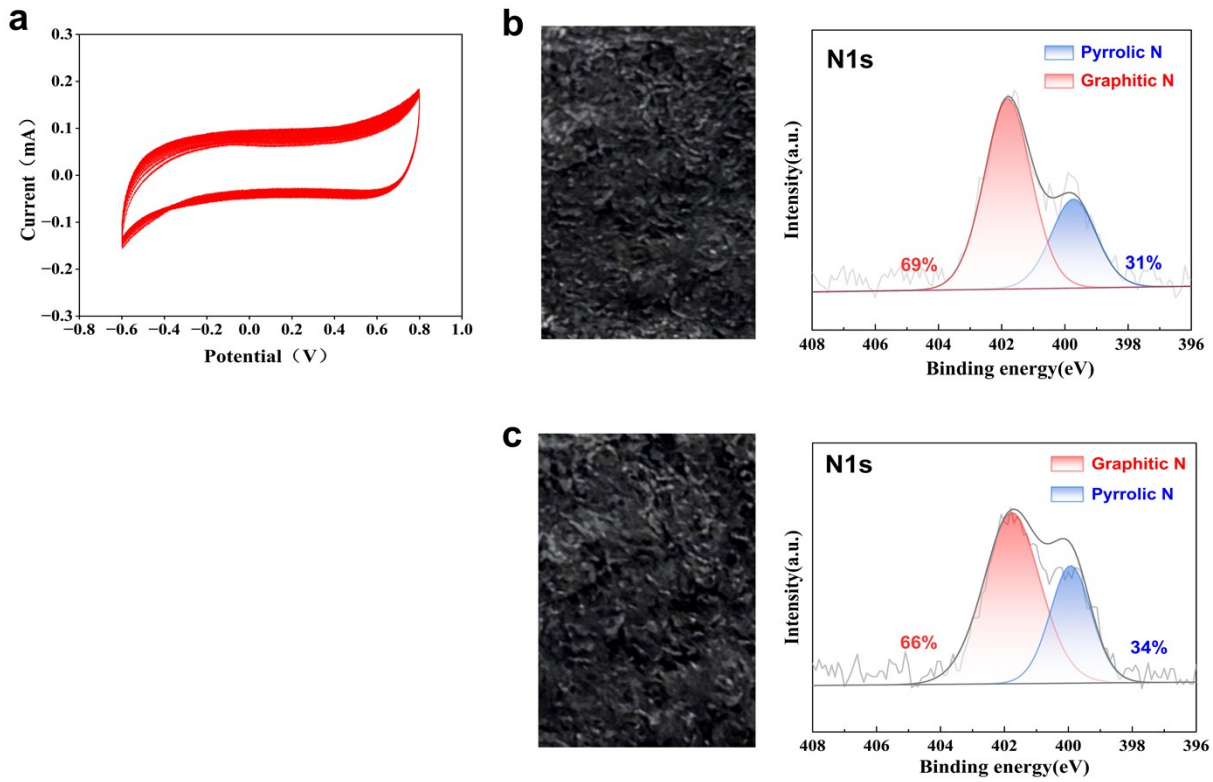

Fig. S18. (a) Cyclic voltammetry curve. Optical photographs and XPS of (b) the sample before and after cyclic voltammetry scan, and(c) the sample after cyclic voltammetry scan.

The sample g-ENGO-1.6 was used as a representative to examine the stability by conducting consecutive cyclic voltammetry (CV) scans for 50 cycles. After that, XPS measurements were conducted. As shown in Fig. S18, the original graphitic-N content (69%) just slightly decreased to 66%. In addition, no significant difference can be found from the optical photos of the sample before and after CV scan. These results demonstrate that the g-ENGO possesses satisfactory electrochemical stability under ORR or OER conditions.

Table S1. Summary of Representative Electrochemical Nitrogen Doping Studies.

Method	Materials	Synthesis Conditions	Nitrogen Source	Total N Content	Nitrogen Species Distribution	Relative Graphitic N Content	Absolute Graphitic N Content	Ref
i-t	Graphite rods	2.2V, 2h, $(C_2H_5NH_3)NO_3/H_2O$=9/1	$(C_2H_5NH_3)NO_3$	2.4%	Pyridinic N:65% Pyrrolic N:35% Graphitic N:0%	0%	0%	(12)
i-t	Graphite rods	7.5V, 5M $CO(NH_2)_2$ and 1M $(NH_4)_2SO_4$	$CO(NH_2)_2$	10.05%	Pyridinic N:30% Pyrrolic N:55% Graphitic N:15%	15%	1.51%	(13)
CV	Pencil Graphite Electrode	0.5V~1.9V, 20 cycles, 5M HNO_3	HNO_3	4.3%	Pyridinic N:15% Pyrrolic N:35% Graphitic N:5% Oxidized N:20% NO_2:25%	5%	0.215%	(14)
i-t	Graphite foil	10V, 1M NH_4NO_3	NH_4NO_3	2.5%	Pyridinic N:30% Pyrrolic N:60% Graphitic	10%	0.25%	(15)

Method	Materials	Synthesis Conditions	Nitrogen Source	Total N Content	Nitrogen Species Distribution	Relative Graphitic N Content	Absolute Graphitic N Content	Ref
					N:10%			
i-t	Graphite rods	6V, 4h, 0.3M $(NH_4)_2SO_4$	$(NH_4)_2SO_4$	5.45%	Pyridinic N:17.72% Pyrrolic N:52.13% Graphitic N:30.15%	30.15%	1.64%	(16)
i-t	Graphite foil	7.5V, 5M $NH_3·H_2O$ and 1M $(NH_4)_2SO_4$	$NH_3·H_2O$	4.95%	Pyridinic N:49.3% Pyrrolic N:45.3% Graphitic N:5.4%	5.4%	0.27%	(17)
i-t	Graphite rods/HOPG	10V, 12h, 3M H_2NCH_2COOH and $NH_3·H_2O$	H_2NCH_2COOH, $NH_3·H_2O$	6.05%	Pyrrolic N:71% Graphitic N:29%	29%	1.75%	(18)
CV	Graphite rods	-5V~5V, 0.006M C_3H_6N6 and 0.1M $(NH_4)_2SO_4$	C_3H_6N6, $(NH_4)_2SO_4$	7.25%	Pyridinic N:26% Pyrrolic N:42% Graphitic N:32%	32%	2.32%	(19)
i-t	Graphite	1.8V,30min,50 wt.%	$(NH_4)_2SO_4$	1.05%	Graphitic	100%	1.05%	This

Method	Materials	Synthesis Conditions	Nitrogen Source	Total N Content	Nitrogen Species Distribution	Relative Graphitic N Content	Absolute Graphitic N Content	Ref
	paper	H_2SO_4; 1.2V,30min,1.25 M $(NH_4)_2SO_4$			N:100%			work

Table S2. Total N, absolute graphitic-N, and relative graphitic-N content in the g-ENGO-x (x represents different oxidation times).

Sample	g-ENGO-0	g-ENGO-5	g-ENGO-10	g-ENGO-20	g-ENGO-30
Total N (%)	1.458	1.6	1.82	2.16	2.6
Absolute graphitic-N (%)	0.5183	0.84	1.259	1.581	1.515
Relative graphitic-N (%)	35	53	69	73	59

Table S3. Total N, absolute graphitic-N, and relative graphitic-N content in g-ENGO-x (x represents different doping potentials)

Sample	g-ENGO-0.8	g-ENGO-1	g-ENGO-1.2	g-ENGO-1.4	g-ENGO-1.6	g-ENGO-1.8
Total N (%)	1.57	1.65	1.05	1.41	1.75	2.37
Absolute graphitic-N (%)	0.9195	0.965	1.05	0.928	1.2043	1.271
Relative graphitic-N (%)	58	59	100	84	69	54

Total N refers to the percentage of all elements in the material, while relative graphitic-N refers to the percentage of total N.

Absolute graphitic-N= Total N*Relative graphitic-N/100

Table S4. Elemental content of EGO after methanol quenching.

Sample	C	O	N	H
Mass %	91.599	0	0.102	8.299

References

1. X. Du, A. Du, D. Wang, Y. Mao, Z. Zhang and W. Xie, Surface-Enhanced Raman Spectroscopic Study of Key Intermediates in Electrochemical Ammonia Decomposition, *Journal of the American Chemical Society*, 2024, **147**, 8083-8087.
2. Y. Li, Y. Hu, F. Shi, H. Li, W. Xie and J. Chen, C−H Arylation on Nickel Nanoparticles Monitored by In Situ Surface-Enhanced Raman Spectroscopy, *Angewandte Chemie International Edition*, 2019, **58**, 9049-9053.
3. Y. Zhao and D. G. Truhlar, The M06 suite of density functionals for main group thermochemistry, thermochemical kinetics, noncovalent interactions, excited states, and transition elements: two new functionals and systematic testing of four M06-class functionals and 12 other functionals, *Theoretical Chemistry Accounts*, 2007, **120**, 215-241.
4. F. Weigend and R. Ahlrichs, Balanced basis sets of split valence, triple zeta valence and quadruple zeta valence quality for H to Rn: Design and assessment of accuracy, *Physical Chemistry Chemical Physics*, 2005, **7**, 3297-3305.
5. M. B. Arvas, M. Gencten and Y. Sahin, One-step synthesized N-doped graphene-based electrode materials for supercapacitor applications, *Ionics*, 2021, **27**, 2241-2256.
6. H. Gürsu, M. Gençten and Y. Şahin, One-step electrochemical preparation of graphene-coated pencil graphite electrodes by cyclic voltammetry and their application in vanadium redox batteries, *Electrochimica Acta*, 2017, **243**, 239-249.
7. C. Jiang, Z. Chen, R. Yang, Z. Luogu, Q. Ren, H. Hu, K. Wang, S. Li, C. Deng, M. Li and L. Zheng, Carbon-Based Flexible Electrode for Efficient Electrochemical Generation of Reactive Chlorine Species in Tumor Therapy, *Advanced Healthcare Materials*, 2025, **14**, 2500369.
8. Q. Shi, W. Tang, K. Kong, X. Liu, Y. Wang and H. Duan, Electrocatalytic Upgrading of Plastic and Biomass-Derived Polyols to Formamide under Ambient Conditions, *Angewandte Chemie International Edition*, 2024, **63**, e202407580.
9. J. Cao, P. He, M. A. Mohammed, X. Zhao, R. J. Young, B. Derby, I. A. Kinloch and R. A. W. Dryfe, Two-Step Electrochemical Intercalation and Oxidation of Graphite for the Mass Production of Graphene Oxide, *Journal of the American Chemical Society*, 2017, **139**, 17446-17456.
10. F. Liu, F. Niu, T. Chen, J. Han, Z. Liu, W. Yang, Y. Xu and J. Liu, One-step electrochemical strategy for in-situ synthesis of S,N-codoped graphene as metal-free catalyst for oxygen reduction reaction, *Carbon*, 2018, **134**, 316-325.
11. H. Wang, W. Guo, B. Liu, Q. Si, H. Luo, Q. Zhao and N. Ren, Sludge-derived biochar as efficient persulfate activators: Sulfurization-induced electronic structure modulation and disparate nonradical mechanisms, *Applied Catalysis B: Environmental*, 2020, **279**, 119361.
12. X. Lu and C. Zhao, Controlled electrochemical intercalation, exfoliation and in situ nitrogen doping of graphite in nitrate-based protic ionic liquids, *Physical Chemistry Chemical Physics*, 2013, **15**, 20005-20009.
13. R. Bhaskaran and R. Chetty, One-Pot Room Temperature Synthesis of Nitrogen-Doped Graphene and Its Application as Catalyst Support for ORR in PEMFCs, *ACS Applied Energy Materials*, 2024, **7**, 390-402.
14. M. B. Arvas, M. Gencten and Y. Sahin, One-step synthesized N-doped graphene-based electrode materials for supercapacitor applications, *Ionics*, 2021, **27**, 2241-2256.
15. A. Shayesteh Zeraati, S. A. Mirkhani, F. Sharif, A. Akbari, E. P. L. Roberts and U. Sundararaj, Electrochemically Exfoliated Graphite Nanosheet Films for Electromagnetic Interference Shields, *ACS Applied Nano Materials*, 2021, **4**, 7221-7233.
16. L. Magerusan, F. Pogacean and S. Pruneanu, Enhanced Acetaminophen Electrochemical Sensing Based on Nitrogen-Doped Graphene, *International Journal of Molecular Sciences*, 2022, **23**, 14866.
17. F. Lou, M. E. M. Buan, N. Muthuswamy, J. C. Walmsley, M. Rønning and D. Chen, One-step electrochemical

synthesis of tunable nitrogen-doped graphene, *Journal of Materials Chemistry A*, 2016, **4**, 1233-1243.

18. Y. Yang, W. Shi, R. Zhang, C. Luan, Q. Zeng, C. Wang, S. Li, Z. Huang, H. Liao and X. Ji, Electrochemical Exfoliation of Graphite into Nitrogen-doped Graphene in Glycine Solution and its Energy Storage Properties, *Electrochimica Acta*, 2016, **204**, 100-107.
19. F. Liu, F. Niu, T. Chen, J. Han, Z. Liu, W. Yang, Y. Xu and J. Liu, One-step electrochemical strategy for in-situ synthesis of S,N-codoped graphene as metal-free catalyst for oxygen reduction reaction, *Carbon*, 2018, **134**, 316-325.